

Concentric Eyewall Typhoon characteristics at Western North Pacific

Yi-Ting Yang¹, Hung-Chi Kuo¹, Eric A. Hendricks², Melinda S. Peng² and Chun-Yen Lee¹

¹Department of Atmospheric Sciences, National Taiwan University,
Taipei, Taiwan, Republic of China

²Naval Research Laboratory, Monterey, CA

1. Introduction

Willoughby et al. (1982) demonstrated the eyewall replacement cycle (ERC) of hurricanes, which is well-known intensity change process. There is large variability associated with intensity change of TC with concentric eyewall (CE) structure (Kuo et al. 2009; Sitkowski et al. 2011). Hawkins and Helveston (2008) itemized different modes of concentric eyewall structure, including the typical ERC, ERCs repeated multiple times, ERC are interrupted by vertical shear and landfall, triple eyewalls, outer eyewall is created at large radius and remains the CE structure for a long time. The varieties of CE evolution have a profound impact of intensity forecast.

This study use microwaves imageries, best track and SHIP datasets to display the structural evolution and intensity change of TCs with CE in Western Pacific between 1997 and 2010.

2. Data and Methodology

The orbital satellite imageries from NRL website are stored as an 800 X 800 pixels color jpeg files that composed with red (R), green (G) and blue (B) colors. We converted every pixel into R, G and B components for all images and deduct the missing areas, the coast lines and coordinate lines. We use JTWC best track data, SSMI and TRMM/TMI 85 GHz microwave imageries, and Statistical Hurricane Intensity Prediction Scheme (SHIPS; DeMaria et al. 2005) for vertical shear and SST data.

We first define the center of typhoons and construct the brightness temperature (Tbb) dataset on polar coordinate system to study the structural changes of eyewall. To minimize the errors that may result from the eye center inaccuracy, we define 5 pixels average in radial direction as 1 bin and a 45-degree sector averaged Tbb profile on the bin data. As a result, there are 8 averaged radial profiles of Tbb. We use four criteria to objectively identify CE structure: (1) $Tbb_{max} \geq \sigma_{outer_min(inner_min)} + Tbb_{outer_min(inner_min)}$; (2) $Tbb_{outer_min} \leq 230K$; (3) more than 5 sectors satisfy the former two conditions, and (4) the distances between two ends of outer rings is smaller than 50 km. We identified 225 CE imageries and 91 CE typhoons

from 1997 to 2010. The detail of method will be reported in Yang et al. (2012).

We exclude the CE cases in which the typhoon center is within 200 km from land in our structural and intensity change study. There are 67 CE cases for the study. We account for the irregular satellite to observation times with regular JTWC best track data by matching the time closet to satellite observation for typhoon's center.

3. Structural and Intensity change

We identify three types of CE structural change: the typical eye replacement cycle (ERC; 53%, 35 cases), the concentric eyewall maintained (CEM; 23.5%, 16 cases) and no typical replacement cycle (NRC; 23.5%, 16 cases). The ERC type is the cases with dissipation of inner core within 20 hr after the CE formation. The CEM type is cases with the CE structure maintained for more than 20 hr (mean duration time is 31 hr for our CEM typhoons). The NRC type is cases with the dissipation of the outer eyewall.

Examples of three types are shown in Fig. 1. We also show two half plane averaged Tbb radial profiles in Fig.1. Of all the possible four separations of the two half plane (as we have 8 45-degree sector), the average profiles shown in Fig. 1 are the ones with the greatest asymmetries. The ordinate of Tbb averaged radial profile is set to decrease upward, so that it resembles somewhat with the typical profile tangential wind. The Tbb profiles display Typhoon Saomai is an ERC cases with inner core dissipated after 12 hrs CE formation. Typhoons Haitang and Ewiniar are NRC cases which maintain the inner eyewall while the outer eyewall disappeared in half. The dissipation of the outer eyewall may be related to the environmental vertical shear or cold ocean surface (Fig. 6 below). Typhoon Winnie, Dianmu and Chaba are CEM cases with large moat width (137 km, 45 km and 65 km, respectively) and outer ring width (137 km, 64 km and 85 km, respectively). These CEM typhoons maintain their CE structure for 46.5, 37.5 and 35.5 hrs, respectively. We also find significant asymmetric convection outside of inner core 8 to 12 hrs before CE formation in most of the cases.

1A.8

To study the structural change in quantitative manner, we compute the parameter of convective area (CA, unit is $K km^2$) as

$$CA = \frac{\pi}{4} \sum_{i=1}^8 \int_{r=0}^{250} (290 - T_r(r)) r dr.$$

Since 290K Tbb is in general without the convection, the CA is the area within 250 km radius weighted with convective activities. The larger value of CA implies more convective activities within the area.

Figure 2 indicates the CA vs Vmax evolution of ERC, NRC and CEM typhoon cases with relevant microwave imageries. The CA of two NRC cases decline dramatically in the outer eyewall dissipation stage. On the other hand, the CA in the ERC cases increases in the eyewall replacement stage. The CA in CEM cases maintains the similar magnitude for a long time.

The Histogram of CE formation intensity is in Fig. 3. It indicates 33 of 67 CE cases form in category 4. In addition, the formation intensity of CEM cases is greater than or equal to category 2, mostly are in category 4 and 5. Figure 4 indicates the composite intensity time series. Figure 4a suggests that a rapid intensity decrease of the NRC cases 12 hr after the CE formation. This may because NRC cases move northward quickly than other cases and experience unfavorable environment (not shown). However, the intensity time series of CEM cases indicates that the intensity is increased and maintained even 24 hr after CE formation. Furthermore, CEM cases composite shows a relative higher intensity for a longer duration than that of Emanuel (2000) and the annular hurricane result from Knaff and Kossin (2003).

The scatter plots of intensity, moat width and outer ring width are shown in Fig. 5. In general, the outer ring width is larger with a larger moat ($R^2=0.5$). Furthermore, CEM cases are with larger moat width (approximately 60 km), strong intensity (approximately $63 ms^{-1}$) and larger outer ring width (approximately 70 km) than that of ERC (averaged intensity, moat size and outer ring width are $59 ms^{-1}$, 40 km and 49 km, respectively) and NRC (averaged intensity, moat size and outer ring width are $60 ms^{-1}$, 44 km and 48 km, respectively) cases. We suspect that the larger moat in the CEM cases may provide the moisture to sustain the inner core convection and shield the inner core from the subsidence induced by the outer ring convections. While the larger moat may stabilize the type II instability across the moat as discussed by Kossin et al. (2000), it may not be

good for the inner core stabilization of the outer vorticity ring. Our result indicates these large moat cases are with very thick outer rings, which may help stabilizing the outer eyewall (Kossin et al. 2000). In the examples of four CEM cases with weaker intensity (category 2 and 3), they have both very large moat (larger than 60 km) and very large outer ring width (larger than 80 km).

4. Environmental condition

Figure 6 is the CE formation locations with CEM, ERC and NRC types indicated by different colors. The tracks 24 hrs before and after the CE formation of CE typhoons are plotted. Note that the NRC cases are with the larger northward translation speed. The triangle symbols are the averaged position. We find that most CEM cases located at west of $140^{\circ}E$. This may be because typhoons in general tend to be more intense in the western part of Pacific after a long journey over ocean. In addition, we find the CEM cases move northward slower than ERC and NRC cases. The northward translation speeds of CEM, ERC and NRC cases are $2.9 m s^{-1}$, $3.4 m s^{-1}$ and $4.8 m s^{-1}$, respectively. Even that most NRC cases start at latitude (north of $18^{\circ}N$) comparable to that of CEM cases, they are farther separated in latitude distance due to the fast northward translation speed of NRC cases.

Figure 7 displays the composited SST and 850mb-200mb vertical shear time series. The NRC cases with large northward translation speed probably is consistent with colder SSTs and larger vertical wind shear encountered (approximately $27^{\circ}C$ and $10.5 ms^{-1}$ in 24 hrs after CE formation, respectively). The unfavorable environment for NRC cases may lead to part of the outer eyewall dissipated. The CEM cases, as expected, are with small vertical wind shear and warmer SSTs (approximately $5 ms^{-1}$ and $29^{\circ}C$, respectively).

5. Summary

We develop an objective method to detect the typhoons with concentric eyewall (CE) structure using the passive microwave satellite SSM/I and TMI imageries. Fourteen years of data with 91 CE typhoons from 1997 to 2010 are studied. The typhoons with centers within 200 km from the land are excluded in our study. Our main results are three types of CE structural change identified: ERC (53%, 35 cases), CEM (23.5%, 16 cases) and NRC (23.5%, 16 cases). The ERC type is the cases with dissipation of inner core within 20 hr after the CE formation. The CEM type is cases with the CE structure

1A.8

maintained for more than 20 hr (mean duration time is 31 hr for CEM typhoons). The NRC type is cases with the dissipation of the outer eyewall. In addition, we find significant asymmetric convection outside of inner core 8 to 12 hrs before CE formation in most of the cases.

We defined the convective area (CA) as the area within 250 km radius weighted with convective activities. The larger value of CA implies more convective activities within the area. After the CE formation, the NRC cases are with faster intensity and CA decline than that of the ERC cases. The CA and intensity in CEM cases maintain the similar magnitude for a long time.

The NRC cases on the average are with a larger northward translation speed of approximately 4.8 ms^{-1} , which is much faster than that of CEM and ERC types (approximately 2.9 ms^{-1} and 3.6 ms^{-1}). As a results, most of the NRC cases occur in the higher latitude, in a relatively low sea surface temperature (approximately 27°C) and in a large vertical shear environment (10.5 ms^{-1} shear between 850 hPa and 200 hPa levels). The CEM cases are often with a greater averaged intensity (63 ms^{-1}), a larger averaged moat size (60 km) and outer ring width (70 km) than that of ERC (averaged intensity, moat size and outer ring width are 59 ms^{-1} , 40 km and 49 km, respectively) and NRC cases (averaged intensity, moat size and outer ring width are 60 ms^{-1} , 44 km and 48 km, respectively). In addition, the CEM cases are in a relative low vertical shear (5 ms^{-1} shear) and a relative high SST (approximately 29°C) environment.

Reference

Hawkins, J. D., and M. Helveston, 2004: Tropical cyclone multiple eyewall characteristics. Preprints, *26th Conf. on Hurricane and Tropical Meteorology*, Miami, FL, Amer. Meteor. Soc., 276–277.

—, —, 2008: Tropical cyclone multiple eyewall characteristics. *28th Conference on Hurricanes and Tropical Meteorology*, Orlando, FL, Amer. Meteor. Soc., 6B.1.

Kossin J. P., W. H. Schubert, and M. T. Montgomery, 2000: Unstable interaction between a hurricane's primary eyewall and a secondary ring of enhanced vorticity. *J. Atmos. Sci.*, **57**, 3893-3917.

Kuo, H.-C., C.-P. Chang, Y.-T. Yang, and H.-J. Jiang, 2009: Western North Pacific typhoons with concentric eyewalls. *Mon. Wea. Rev.*, **137**, 3758-3770.

Sitkowski, M., J. P. Kossin, and C. M. Rozoff: Intensity and structure changes during hurricane eyewall replacement cycles. *Mon. Wea. Rev.* in press.

Willoughby, H. E., and M. B. Chelmon, 1982: Objective determination of hurricane tracks from aircraft observations. *Mon. Wea. Rev.*, **110**, 1298-1305.

Yang, Y.-T., H.-C. Kuo, C.-H. Liu and C.-P. Chang, 2012: A objective method for concentric eyewalls recognition with SSM/I and TMI satellite data. (in preparation)

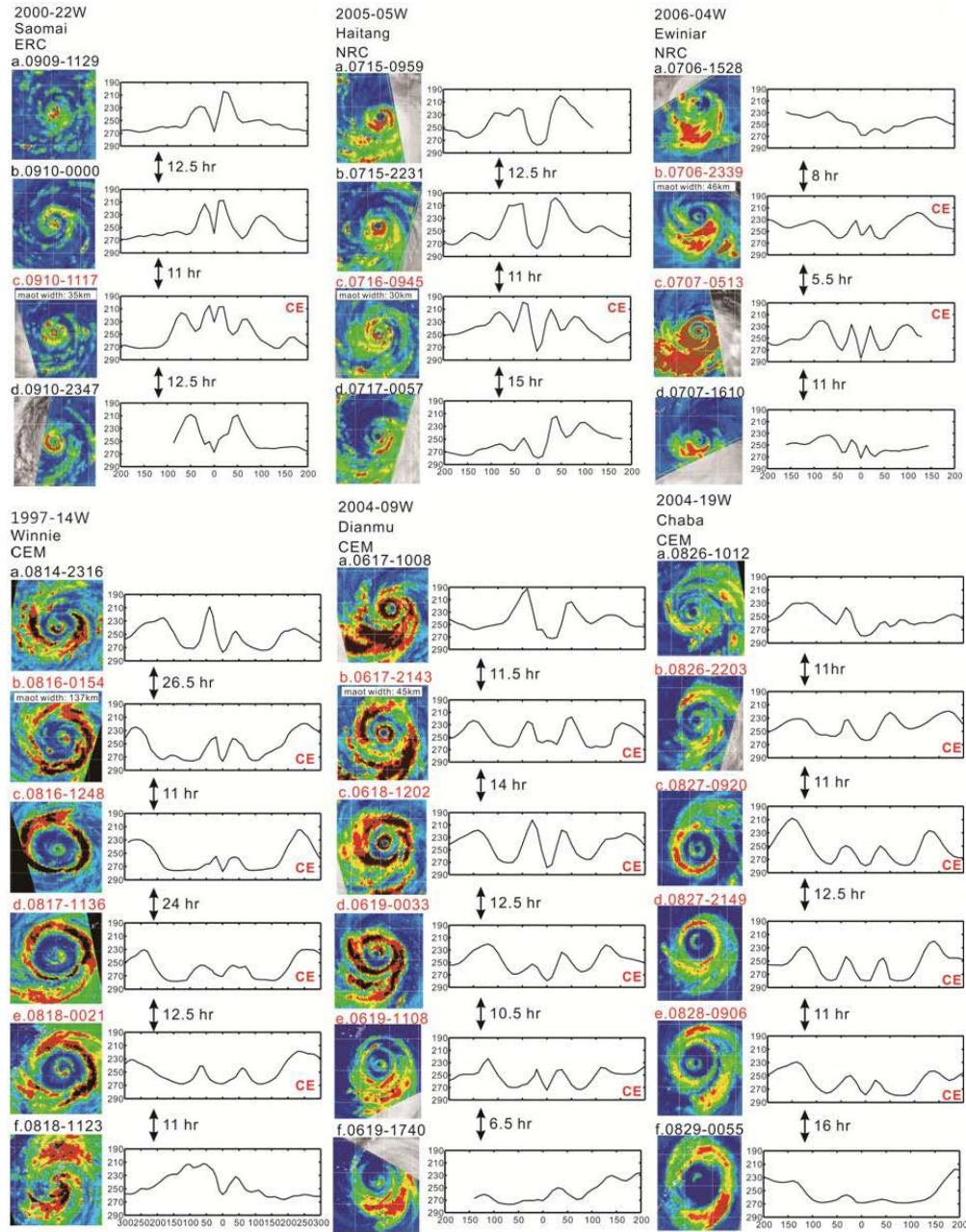


Figure 1: The imagery sequences and averaged Tbb radial profile of Typhoon Saomai 2000 (ERC), Haitang 2005(NRC), Ewiniar 2006 (NRC), Winnie 1997(CEM), Dianmu 2004(CEM) and Chaba 2004(CEM).

1A.8

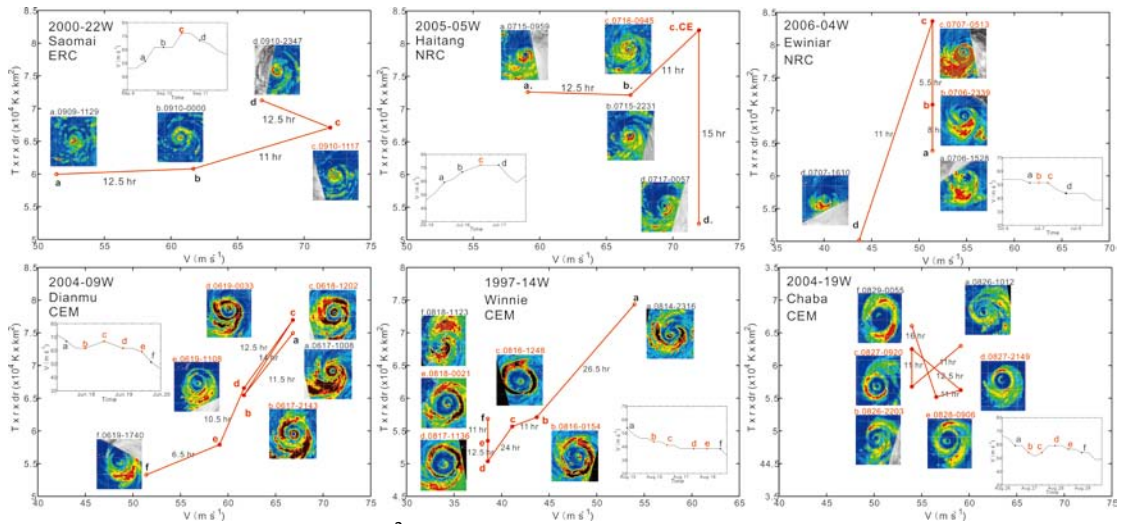


Figure 2: The convective area ($K km^2$) vs V_{max} evolution of ERC, NRC and CEM typhoon cases with relevant microwave imageries.

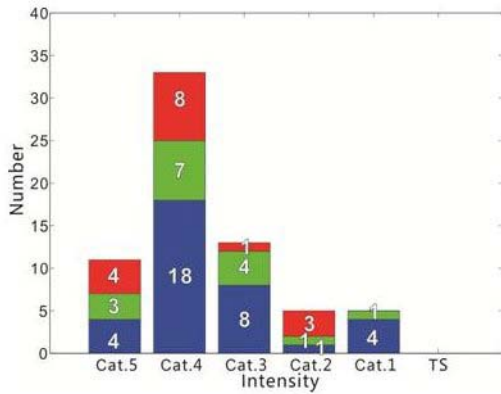


Figure 3: Histogram of the concentric cases against the intensity as categorized by the Saffir–Simpson scale. Blue, green and red are indicated ERC, NRC and CEM, respectively.

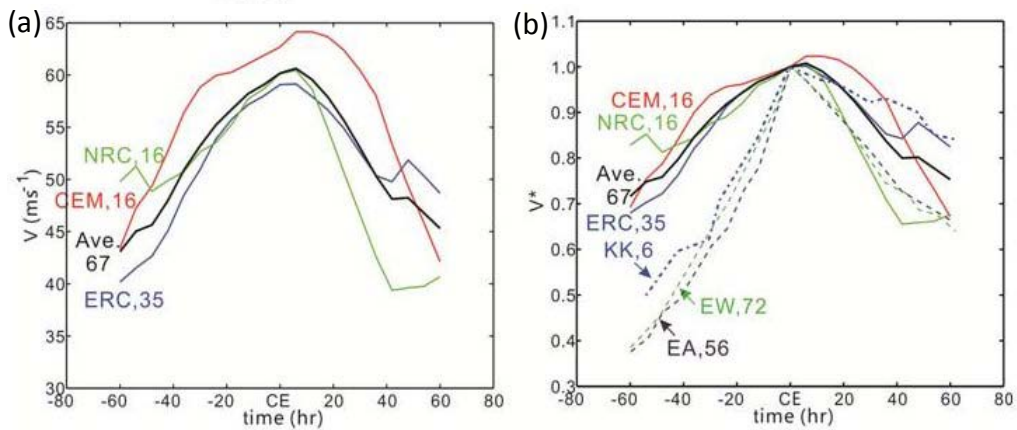


Figure 4: (a) Composite time series of the intensity; (b) as (a) but normalized intensity and also plotted are the average tropical cyclones in the Atlantic and western North Pacific that did not encounter cold water or make landfall as reported by Emanuel (2000, EA and EW indicate Atlantic and Pacific, respectively) and annular hurricanes as reported by Knaff and Kossin (2003, KK).

1A.8

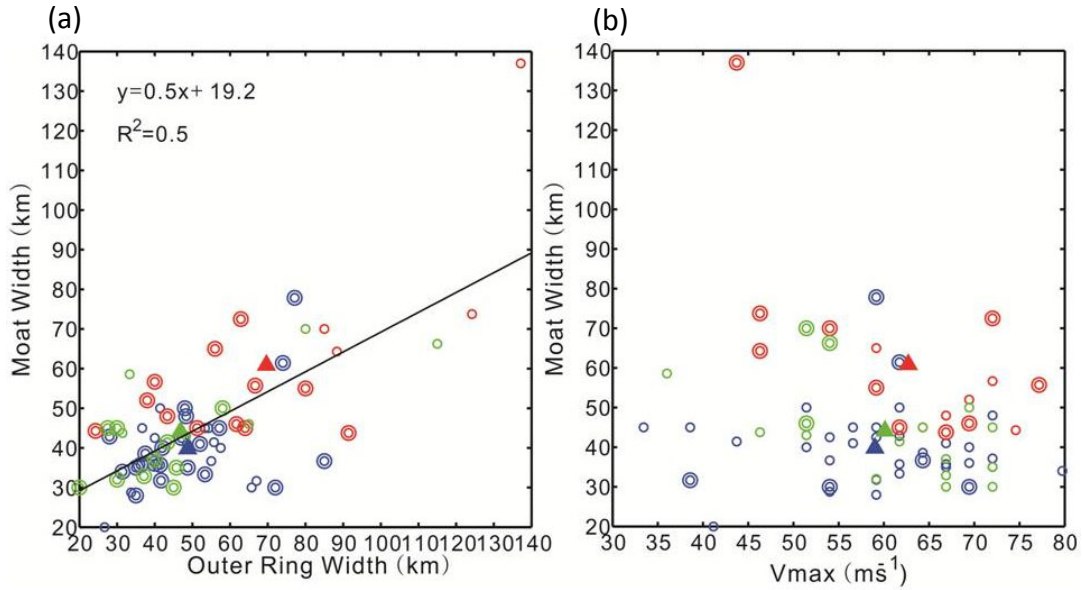


Figure 5: (a) The moat width vs outer ring width. The double circle means the intensity greater than or equal to category 4; (b) The moat width vs intensity. The double circle means the outer ring width greater than or equal to 60 km. Blue, green and red are indicated ERC, NRC and CEM, respectively. The triangle signals indicate average value.

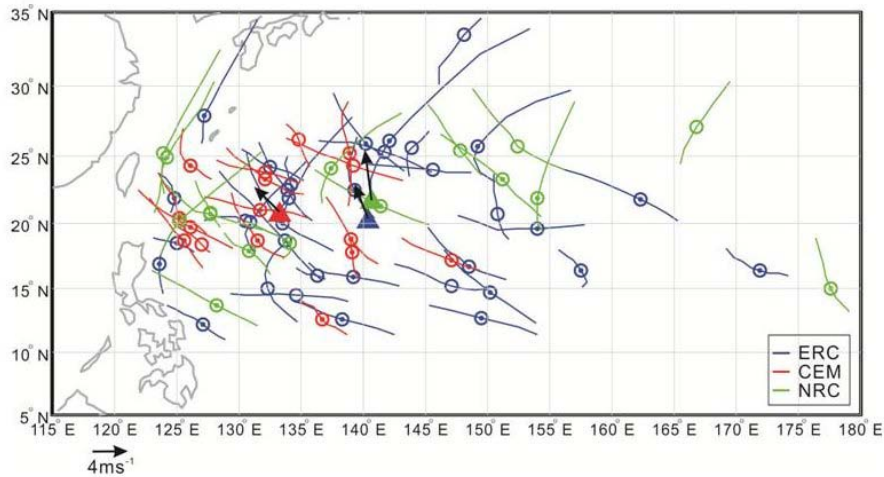


Figure 6. The CE formation locations with CEM, ERC and NRC types indicated by red, blue and green colors, respectively. The tracks 24 hrs before and after the CE formation of CE typhoons are shown. Note that the NRC cases are with the larger northward translation speed. The triangle symbols are the averaged position.

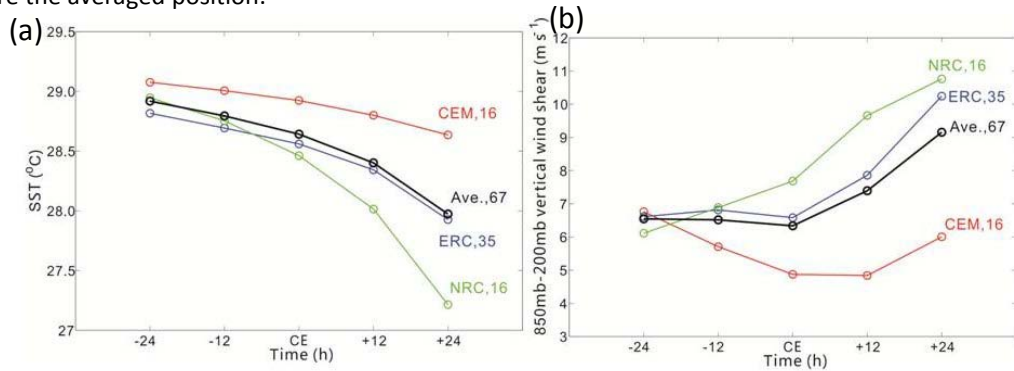


Figure 7. (a) The SST and (b) 850mb-200mb vertical wind shear ($m s^{-1}$) time series of CEM (red), NRC (green) and ERC (blue) cases.